JOURNAL OF CATALYSIS 113, 341–352 (1988)

Analysis of CO Hydrogenation Pathways Using the Bond-Order-Conservation Method

EVGENY SHUSTOROVICH* AND ALEXIS T. BELL†

Corporate Research Laboratories, Eastman–Kodak Company, Rochester, New York 14650, and †Materials and Molecular Research Division, Lawrence Berkeley Laboratory, and Department of Chemical Engineering, University of California, California 94720-9989

Received March 10, 1987; revised March 29, 1988

The bond-order-conservation (BOC) method has been used to identify the energetics associated with the hydrogenation of CO over (111) surfaces of Ni, Pd, and Pt. In the formation of CH_4, the C–O bond of CO is cleaved. BOC calculations for Ni indicate that cleavage of the C–O bond occurs primarily by direct dissociation of molecularly adsorbed CO. The activation energy for direct dissociation of CO on Pd and Pt is significantly greater than that for hydrogen assisted dissociation, and hence the latter process is more significant. The BOC calculations indicate that for these metals the species from which C–O bond cleavage occurs is CH_3O_s. Because the activation barriers for CH_3O_s dissociation and hydrogenation to form CH_3OH are close for Pd and Pt, these metals are effective catalysts for both CH_4 and CH_3OH synthesis. By contrast, the BOC method predicts that CH_4 should be the principal product formed over Ni.

INTRODUCTION

Considerable attention has been dedicated in recent years to understanding the mechanism by which methane and methanol are formed from carbon monoxide and hydrogen over Group VIII metals (*1–5*). The results of experimental studies indicate that C–O bond cleavage is a critical step in the synthesis of methane. While some authors have suggested that this process occurs via dissociation of adsorbed CO, others have provided evidence that C–O bond cleavage occurs from a partially hydrogenated form of CO (e.g., HCO, H_2CO, CH_3O). There are also indications from studies of the H_2/D_2 isotope effect on CO hydrogenation that the extent of hydrogenation prior to C–O bond breakage is a function of metal composition (*6*). In contrast to methane synthesis, isotopic tracer studies of methanol synthesis indicate that CO hydrogenation proceeds without rupture of the C–O bond (*7*). A number of investigations have also shown that the selectivity of methanol formation is highest over metals such as Pd, Pt, and Rh which do not favor CO dissociation and lowest over metals such as Ni, Fe, and Ru which more readily dissociate CO (*8*).

The aim of this study was to address, theoretically, some fundamental aspects of CO hydrogenation. We were interested primarily in the following three questions:

1. Does C–O bond cleavage during the synthesis of methane involve the participation of adsorbed hydrogen and if so, how does metal composition influence the extent to which hydrogen participates?
2. What are the primary energy barriers to methane and methanol formation and how does their magnitude depend on metal composition?
3. What are the energy profiles of possible pathways for methane and methanol synthesis?

For the sake of comparison we have examined these questions for the representative platinum group metals Ni, Pd, and Pt.

As a theoretical framework, we have used the bond-order-conservation (BOC) method (*9, 10*) to calculate the activation energies of elementary steps involved in the

0021-9517/88 $3.00

hydrogenation of CO to methane and methanol, as well as the heats of adsorption of all relevant reaction intermediates. Previous experience with the BOC method has shown (*9, 10*) that it can provide heats of adsorption for molecular species, which are in good agreement with the values observed experimentally. This approach has also proven effective for predicting the activation energies for relatively simple processes such as NO decomposition and CO oxidation (*9f*). The results of the present study show that the BOC method can provide insights into the energetics of CO hydrogenation and the dependence of reaction pathways on metal composition. An extension of the present approach to the transformations of C_2H_x ($x = 0$–6) species on metal surfaces will be given elsewhere (*11*).

THE BOC METHOD

The basic assumptions and the mathematical formalism of the BOC method are described in detail in Refs. (*9a–h*) and reviewed in Ref. (*10*). The reader is referred to these publications for any questions of methodology as well as the qualitative validity and quantitative accuracy of the BOC projections.

An important product of the BOC method is a set of analytical expressions for estimating the activation barriers for dissociation and recombination of reactants and possible intermediates of surface reactions. All the relations are expressed in terms of atomic (for the atoms directly coordinated to a surface) or molecular heats of chemisorption, Q. In the latter case, Q may be for the whole molecule or the polyatomic fragments, into which the molecule dissociates. The important point is that within the BOC framework the atomic and molecular heats of chemisorption are not independent entities but are interrelated via the molecular gas-phase bond energies, total or partial, depending on the case (*9, 10*).

Given below is a brief summary of the basic BOC equations for the zero-coverage limit. On flat, symmetric metal surfaces with an M_n unit mesh, adatoms (A) always occupy the highest coordination (hollow) sites. The corresponding heat of chemisorption is given by

$$Q_A = Q_{oA}(2 - 1/n), \tag{1}$$

where Q_{oA} is the maximum two-center M–A bond energy for the on-top site. For a linearly monocoordinated admolecule (M–A–B), the heat of molecular chemisorption is

$$Q_{AB} \leq \frac{Q_{oA}^2}{Q_{oA} + D_{AB}}, \tag{2}$$

where D_{AB} is the gas-phase dissociation energy and Q_{oA} is from Eq. (1). The inequality sign reflects neglect of a small negative contribution from the M–B interaction. In the same approximation, the n-fold M_n–AB coordination will have the bond energy (*9, 10*)

$$Q_{AB,n} \leq \frac{Q_{oA}^2}{(Q_{oA}/n) + D_{AB}} \quad \text{for } D_{AB} > \frac{n-1}{n} Q_{oA}. \tag{3}$$

In this case, however, the neglected negative M_n–B contribution is larger in absolute value than that for M–B, so that all the AB chemisorption sites tend to be close in energy, the approximation $Q_{AB} \simeq Q_{AB,n}$ becoming more accurate the larger the value of D_{AB}.

For dicoordination of AB, the bridge di-σ (M  M) mode appears to be the general bonding prototype and the bonding energy is given by (*9g*)

$$Q_{AB} = \frac{ab(a+b) + D(a-b)^2}{ab + D(a+b)}, \tag{4}$$

where

$$a = Q_{oA}^2(Q_{oA} + 2Q_{oB})/(Q_{oA} + Q_{oB})^2,$$

$$b = Q_{oB}^2(Q_{oB} + 2Q_{oA})/(Q_{oA} + Q_{oB})^2,$$

and $D = D_{AB}$.

In the homonuclear case, $a = b$ and Eq. (4)

is reduced to

$$Q_{A_2} = \frac{(9/2)Q_{oA}^2}{3Q_{oA} + 8D_{A_2}}. \quad (5)$$

Equations (2)–(4) can be applied to polyatomic adspecies such as AB_x or ZZ' ($Z,Z' = B_x$ or AB_x). For the case of monocoordination (M_n–AB_x) the bond dissociation energy D_{AB} in Eqs. (2) and (3) is replaced by D_{AB_x}, the total bond energy of AB_x in the gas phase. For dicoordination (M 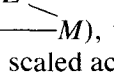 M), the values of a, b, and D must be scaled according to the nature of Z *and* Z'. This point is best illustrated by example. If CH_2CH_2 is coordinated via both carbon atoms, then $Z = Z' = CH_2$. In this case Q_{oA} in Eq. (4) represents the bonding energy of atomic carbon for an on-top site (i.e., $Q_{oC} = Q_C/(2 - 1/n)$) and D_{A_2} is the total energy of all bonds formed by each C atom, namely $D_{A_2} = 355$ kcal/mol (*9g*). Chemisorption of unsymmetric molecules, such as $O{=}CH_2$, can still be described by Eq. (4). In this case $Q_{oA} = Q_{oO}$, $Q_{oB} = Q_{CH_2}$ for an on-top site, and D represents the energy of the C=O bond, $D_{C=O}$. To calculate $D_{C=O}$ requires a partitioning of the total bond energy, D_{H_2CO}, into the relevant two-center contributions (i.e., $D_{H_2CO} = D_{H_2C} + D_{C=O}$). As discussed in Refs. (*9f–h, 11*), this procedure involves some arbitrariness. One can, nevertheless, define a reasonable procedure for doing the partitioning, which is illustrated in the Appendix.

From Eqs. (1)–(5), it clearly follows that the molecular heat of chemisorption Q_{ZZ}, rapidly decreases as the gas-phase dissociation (total bond) energy of ZZ' increases, Q_{ZZ}, being typically smaller than the relevant atomic heats of chemisorption by a factor of 5–10 or even 15 (*9, 10*). For example, on Ni(111), $Q_{C_2H_4} \simeq 12$ kcal/mol compared to $Q_C \simeq 170$ kcal/mol (*9g*). For this reason, the periodic changes in Q_{ZZ}, for molecules ZZ' such as CO, CH_3, NH_3, NO, H_2O, C_2H_4, C_2H_2 are small compared to the large variations in Q_A observed for the relevant multiply bonded adatoms A (*10*).

If a diatomic molecule AB approaches a surface from the gas phase, the activation barrier $\Delta E^*_{AB,g}$ for dissociation $AB_g \rightarrow A_s + B_s$ explicitly depends on the atomic chemisorption energies, Q_A and Q_B, namely (*9b, 10*)

$$\Delta E^*_{AB,g} = D_{AB} - (Q_A + Q_B) + \frac{Q_A Q_B}{Q_A + Q_B}. \quad (6)$$

For homonuclear dissociation $A_{2,g} \rightarrow A_s + A_s$, Eq. (6) reduces to

$$\Delta E^*_{A_2,g} = D_{A_2} - \tfrac{3}{2}Q_A \quad (7)$$

in good agreement with experiment (*10*). Obviously, the dissociation barrier $\Delta E^*_{AB,s}$ from a chemisorbed state will be larger exactly by the amount of the molecular heat of chemisorption Q_{AB},

$$\Delta E^*_{AB,s} = \Delta E^*_{AB,g} + Q_{AB}. \quad (8)$$

For the reverse reaction of recombination of chemisorbed A_s and B_s, the activation barrier is (cf. Eq. (6))

$$\Delta E^*_{A-B} = \frac{Q_A Q_B}{Q_A + Q_B} \quad (9)$$

so that

$$\Delta E^*_{A-A} = \tfrac{1}{2}Q_A. \quad (10)$$

It should be noted that while Eqs. (8) and (9) were derived originally to account for the recombination of atomic species, these equations can be applied to polyatomic fragments as well, as will be discussed below.

Another point of note is that the activation barrier for recombination cannot be smaller than $\Delta H = \Delta H_{AB} - \Delta H_{A+B}$, the difference between the enthalpies of the reactant AB_s ($-\Delta H_{AB} = D_{AB} + Q_{AB}$) and the products A_s and B_s ($-\Delta H_{A+B} = Q_A + Q_B$). Thus, the BOC barrier [eq. (9)] is only the *necessary* (minimal energy) condition for recombination, which may be *sufficient* if

$$\frac{Q_A Q_B}{Q_A + Q_B} \geq \Delta H = Q_A + Q_B - D_{AB} - Q_{AB} \quad (11)$$

but may *not* be sufficient if

$$\frac{Q_A Q_B}{Q_A + Q_B} < \Delta H = Q_A + Q_B - D_{AB} - Q_{AB}. \quad (12)$$

In the last case, we will assume the recombination barrier to be the enthalpy difference ΔH (*9h*).

The BOC relations given above all correspond to the case of zero adsorbate coverage. In reality, however, most heterogeneously catalyzed reactions are carried out under conditions where a substantial fraction of the catalyst surface is covered by adsorbed species. In our previous work (*9c, 9e, 10*) we have shown that heats of chemisorption and activation barriers are affected by surface coverage in a complex, nonlinear fashion. Depending on the nature of the adsorbate, the heat of chemisorption can either increase or decrease. The resulting changes in the activation barriers, for both dissociation and recombination from a chemisorbed state [cf. Eqs. (8) and (9)], will tend to compensate to some extent, although reliable quantitative estimates are not possible at present. As a consequence, we will proceed with zero-coverage estimates in the hope that they qualitatively reflect the relative energetics of elementary steps composing the reaction mechanism under the steady-state conditions.

One further point must be made before we proceed to examine the results of our calculations. The velocity at which a given elementary process takes place is described by the parameter k, which can, in turn, be described by a preexponential factor A and an activation energy ΔE^*, such that

$$k = A \exp(-\Delta E^*/RT). \quad (13)$$

Clearly, in order to make a meaningful comparison between two reactions based solely on the values of ΔE^*, it is necessary that the values of A be approximately the same. This condition is most likely to be met for the specified reaction taking place on a given surface of two different metals (i.e., Pt(111) and Ni(111)). The second-best case to consider is two reactions of the same order differing by one reactant only, for example, $C_s + H_s \rightleftarrows CH_s$ vs $CH_s + H_s \rightleftarrows CH_{2,s}$. Finally, if a vacant surface site S is treated as a reactant, one can compare dissociation reactions with recombination reactions, e.g., $S + CO_s \rightleftarrows C_s + O_s$ vs $H_s + CO_s \rightleftarrows HCO_s + S$. Here, however, the conclusions based solely on ΔE^* will be the least definitive, since the differences in the nature of surface sites (on-top, bridge, hollow) and in the effective number of the sites involved in the reaction may strongly affect the value of A.

RESULTS

Table 1 summarizes the zero-coverage heats of chemisorption on Ni(111), Pd(111), and Pt(111). For adatoms H, O, and C, the experimental values of Q_A were used, except for Q_C for Pd and Pt, which are unknown and therefore were interpolated (*9g, 9h*). The values of Q for molecules and molecular fragments comprising C, O, and H were calculated, except for CO, where reliable experimental data are available. As we have found earlier (*9f*), all the AB_x species should be monocoordinated via one atom A, M_n–AB_x, where the optimal value of n decreases as D_{AB_x} decreases (*9f, 10*). For formyl the monocoordination via C is also much more favorable (by ~15 kcal/mol) than the dicoordination via both C and O. For formaldehyde and monocoordination via O and dicoordination via both C and O are very close in energy, the preference depending on metal composition (*9f, 9g*). Because of this, we have used only the set of Q's for monocoordination.

Where comparison with experimental data is possible, the accuracy of the heats of adsorption predicted by the BOC theory is found to be reasonably good. For example, the value of Q_{CH_4} listed in Table 1 is 10 kcal/mol for Ni(111) and Pd(111), and 9 kcal/mol for Pt(111). These values compare favorably with the experimentally observed

TABLE 1

Initial Heats of Chemisorption (Q) and Total Bond Energies in the Gas Phase (D) and in Chemisorbed States ($D + Q$) on Ni(111), Pd(111), and Pt(111)[a]

Species	D[b]	Ni(111)		Pd(111)		Pt(111)	
		Q[c]	$D+Q$	Q[c]	$D+Q$	Q[c]	$D+Q$
C	—	171	171	160	160	150	150
CH	81	90	171	82	163	73	154
CH_2	183	44	227	40	223	36	219
CH_3	293	26	319	24	317	21	314
CH_4	398	10	408	10	408	9	407
H	—	63	63	62	62	61	61
O	—	115	115	87	87	85	85
OH	102	38	140	23	125	22	124
OH_2	220	17	237	11	231	10	230
OCH_3	383	43	426	25	408	24	407
CH_3OH	487	15	502	12	499	11	498
CO	257	27	284	34	291	32	289
HCO[d]	274	28	302	25	299	22	296
		13	287	8	282	7	281
COH	233[e]	55	288	50	283	44	277
H_2CO	361	19	380	12	373	11	372

[a] All energies in kilocalories per mole.
[b] Reference (*12*).
[c] See text for the relevant formulas and explanations.
[d] The first line corresponds to monocoordination via C, the second line to dicoordination via both C and O.
[e] Reference (*13*).

value of 6 kcal/mol for polycrystalline Rh (*14*). In the case of H_2O, we report in Table 1 a value of Q_{H_2O} = 10 kcal/mol for Pt(111). The experimentally observed value on this surface is 15 kcal/mol (*15*). The agreement here is better than one might first imagine when it is recalled that even at low coverages of H_2O, hydrogen bonds are formed which raise the heat of adsorption by ~3 kcal/mol per bond (*16*) over that for an isolated H_2O molecule. The agreement between theory and experiment is particularly good for CH_3OH. Table 1 lists values of Q_{CH_3OH} of 15 and 11 kcal/mol for Ni(111) and Pt(111), respectively, whereas the corresponding values observed experimentally are 14 and 12 kcal/mol (*17, 18*). Finally, for H_2CO, values of 9, 12, and 11 kcal/mol are listed for Q_{H_2CO} for Ni(111), Pd(111), and Pt(111), respectively. Experimental values for Q_{H_2CO} on these metals have not been reported but a value of 15 kcal/mol has been determined for Ru(0001) (*19*).

Tables 2 and 3 list the activation energies predicted for various elementary reactions believed to be involved in the synthesis of CH_4 and CH_3OH. With the exception of CO and CH_4 dissociation, a comparison of the predicted barrier heights with those determined experimentally is not possible, since

TABLE 2

Initial Activation Barriers for Forward (ΔE_f^*) and Reverse (ΔE_r^*) Elementary Reactions for Methanation on Ni(111), Pd(111), and Pt(111)[a]

	Reaction	ΔE_f^*			ΔE_r^*		
		Ni	Pd	Pt	Ni	Pd	Pt
1.	$CO_s \rightleftarrows C_s + O_s$	67	100	108	69	56	54
2.	$H_s + C_s \rightleftarrows CH_s$	63	59	57	0	0	0
3.	$H_s + CH_s \rightleftarrows CH_{2,s}$	33	31	27	26	29	31
4.	$H_s + CH_{2,s} \rightleftarrows CH_{3,s}$	12	11	9	41	43	43
5.	$H_s + CH_{3,s} \rightleftarrows CH_{4,g}$	6	5	4	22	24	27
	$H_s + CH_{3,s} \rightleftarrows CH_{4,s}$	6	5	4	32	34	36
6.	$H_s + CO_s \rightleftarrows HCO_s$[b]	48	57	56	3	3	2
7.	$HCO_s \rightleftarrows CH_s + O_s$	73	98	106	57	49	49
8.	$HCO_s \rightleftarrows COH_s$	14	16	19	0	0	0
9.	$COH_s \rightleftarrows C_s + OH_s$	28	40	44	51	42	41
6 + 8 + 9.[c]	$H_s + CO_s \rightleftarrows C_s + OH_s$	87–90	110–113	117–119	51–54	42–45	41–43

[a] All energies in kilocalories per mole. See text for the relevant formulas and explanations.
[b] For monocoordination via C.
[c] The range of ΔE^* is due to the nonzero values of ΔE_r^* for reaction (6).

TABLE 3

Zero-Coverage Activation Barriers for Forward (ΔE_f^*) and Reverse (ΔE_r^*) Elementary Reactions for Methanol Formation on Ni(111), Pd(111), and Pt(111)[a]

	Reaction	ΔE_f^*			ΔE_r^*		
		Ni	Pd	Pt	Ni	Pd	Pt
1.	$CO_s + H_s \rightleftarrows HCO_s$[b]	48	57	56	3	3	2
2.	$HCO_s + H_s \rightleftarrows H_2CO_s$	19	18	16	34	30	31
3.	$H_2CO_s \rightleftarrows CH_{2,s} + O_s$	70	90	93	32	27	25
4.	$H_2CO_s + H_s \rightleftarrows CH_3O_s$	43	39	38	26	12	12
5.	$CH_3O_s \rightleftarrows CH_{3,s} + O_s$	13	23	25	21	19	17
6.	$CH_3O_s + H_s \rightleftarrows CH_3OH_g$	26	18	17	24	35	36
	$CH_3O_s + H_s \rightleftarrows CH_3OH_s$	26	18	17	39	47	47
7.	$CH_3OH_g \rightleftarrows CH_{3,s} + OH_s$	42	56	59	15	12	11
	$CH_3OH_s \rightleftarrows CH_{3,s} + OH_s$	57	68	70	15	12	11

[a] All energies in kilocalories per mole. See text for the relevant formulas and explanations.

[b] For monocoordination via C.

the experimental data are not available. In the case of CO dissociation on a Ni(111) surface, our calculations yield a value of $\Delta E^*_{CO,g} = 40$ kcal/mol. This value is in reasonably good agreement with the experimental estimate of 30–40 kcal/mol obtained from recent molecular beam studies (*20a*). For CH_4 dissociative adsorption from the gas phase, the BOC method predicts $\Delta E^*_{CH_4,g} = 22$ kcal/mol, whereas recent molecular beam studies (*20b*) suggest that the activation energy is ≥ 18 kcal/mol.

While the agreement between theory and experiment reported above does not guarantee the accuracy of the remaining barrier heights listed in Tables 2 and 3, there are reasons to believe that the BOC method (Eqs. (6)–(10)) does provide acceptable values. For example, in our previous studies (*9f*), of the reaction $CO_s + O_s \rightarrow CO_{2,s}$, the BOC method yields values of $\Delta E^*_{CO,s} = 23$, 24, and 24 kcal/mol for Pt(111), Pd(111), and Rh(111), in good agreement with the experimentally observed values of 25, 25, and 27 kcal/mol, respectively. We have also found (*9f*) that for the reaction $CO_{2,g} \rightarrow CO_s + O_s$ on Rh(111), the BOC method gives $\Delta E^*_{O(CO)} = 17$ kcal/mol, which is indistinguishable from the experimentally observed value (*21*).

DISCUSSION

Energy profiles for the synthesis of CH_4 can be constructed from the activation energies for elementary reaction steps listed in Tables 2 and 3. Illustrations of such profiles are given in Figs. 1 and 2 for Ni and Pd, respectively. For the sake of convenience, the energy scale in these figures has been set to zero for the case of CO coadsorbed with four H atoms. Since the heats of chemisorption of reactants and products and the activation energies of elementary steps are nearly identical for Pd and Pt, the energy profiles for Pt are nearly the same as those for Pd, and for this reason are not shown.

Figures 1 and 2 each show three reaction networks. The common feature of each network is rupture of the C–O bond at some step prior to the final one in which CH_4 is formed. For pathway A, the C–O bond rupture occurs by dissociation of CO_s, whereas for pathways B and C, the C–O bond is broken by dissociation of HCO_s and CH_3O_s groups, respectively. A fourth possibility involving dissociation of adsorbed H_2CO_s is excluded, since the activation energy for this step (see Table 3) is significantly larger than that for the hydrogenation of H_2CO_s to CH_3O_s.

Inspection of Figs. 1 and 2 reveals a number of interesting points. For both Ni and Pd, the activation barrier for producing C_s via direct dissociation of CO_s is lower than that for producing C_s via the dissociation of HCO_s. It should be noted, though, that the difference in barrier heights is smaller for Pd than for Ni. For both metals the activation barrier for HCO_s hydrogenation is significantly lower than that for HCO_s dissociation into CH_s and O_s, and as a consequence the formation H_2CO_s should be the preferred process. Since the activation barrier for H_2CO_s dissociation into $CH_{2,s}$ and O_s is higher than that for the hydrogenation of H_2CO_s to CH_3O_s (see Tables 2 and 3), the latter process ought to occur more readily. Once formed, CH_3O_s can dis-

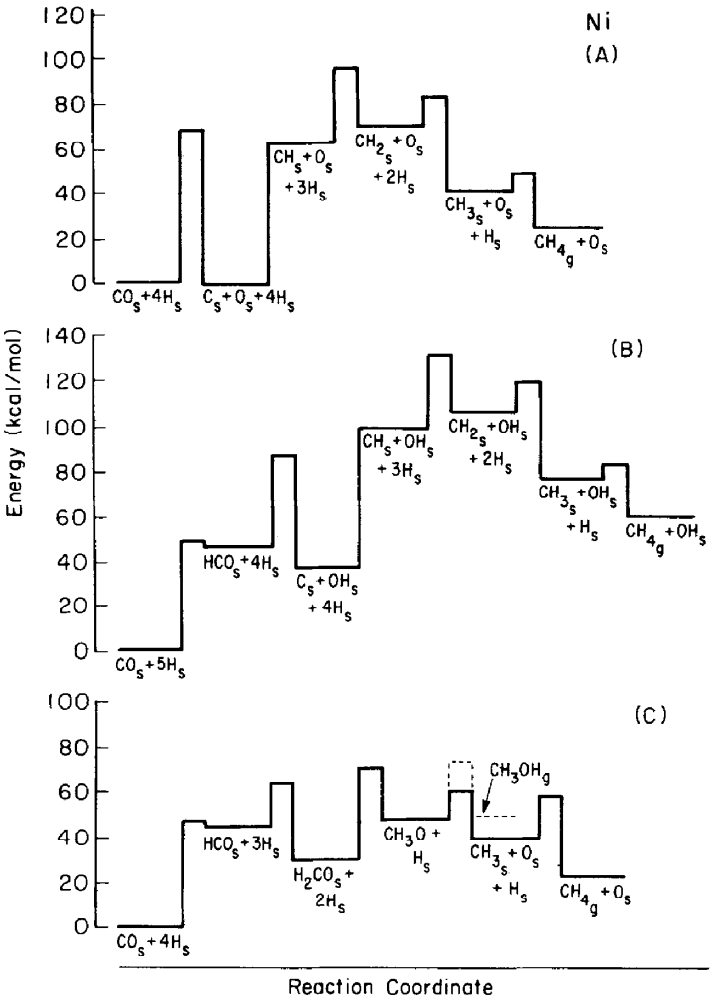

FIG. 1. Potential energy diagrams for the hydrogenation of CO on Ni(111).

sociate to produce $CH_{3,s}$ and O_s or add hydrogen to produce CH_3OH. For Ni, the activation energy for CH_3O_s dissociation into $CH_{3,s}$ and O_s is lower than that for CH_3O_s hydrogenation to CH_3OH, but the reverse is true for Pd.

The preceding analysis allows us to predict on the basis of energetic considerations at which point C–O bond rupture is most likely to occur during the synthesis of CH_4. In the case of Ni, it is evident that cleavage of the C–O bond should occur preferentially via dissociation of CO_s, and to a lesser extent via dissociation of CH_3O_s. In the case of Pd (or Pt by virtue of the similarity in the energetics for Pd and Pt), it is unlikely that C–O bond rupture takes place via CO dissociation because of the very high activation energy for this step. Instead, Fig. 2 indicates that the energetically preferred reaction would be the dissociation of CH_3O_s into $CH_{3,s}$ and O_s.

The present calculations also provide insights into the energetics of hydrogenation of adsorbed carbon. Table 2 and Figs. 1 and 2 show that the addition of a hydrogen atom to carbon to form a methylene group is strongly endothermic, whereas the subsequent hydrogenation of methyne to methylene is weakly endothermic. By contrast,

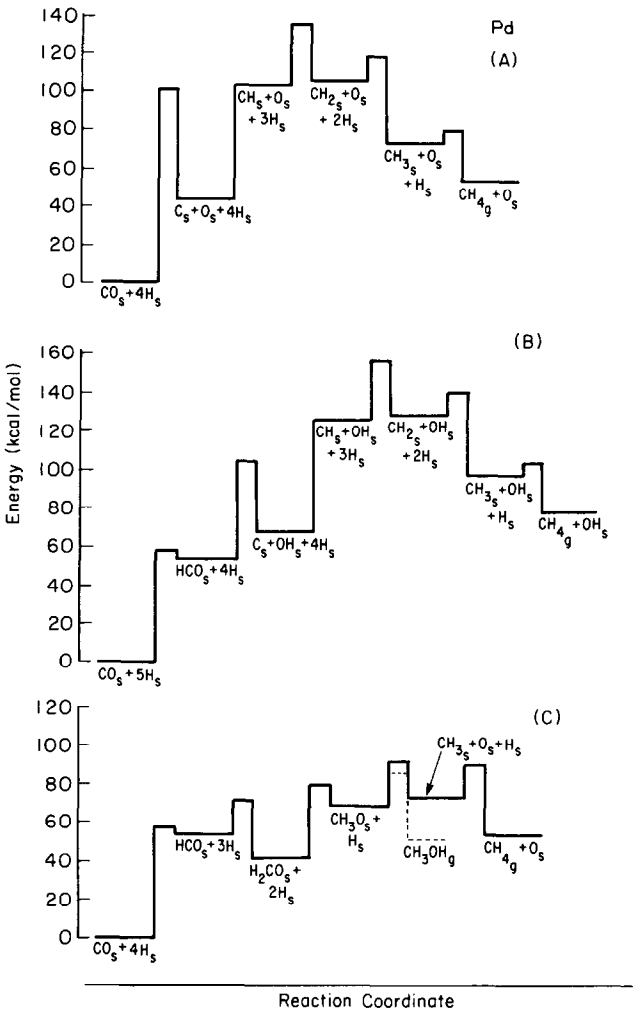

FIG. 2. Potential energy diagrams for the hydrogenation of CO on Pd(111).

the hydrogenation of methylene to methyl and the reductive elimination of methyl as methane are both exothermic processes. It is significant to note, though, that because of the high endothermicity of the first step (i.e., $C_s + H_s \rightarrow CH_s$), the heat of reaction for the overall process $C_s + 4H_s \rightleftarrows CH_{4_g}$ is mildly endothermic for Ni and Pd (ΔH_{Ni} = 35 kcal/mol and ΔH_{Pd} = 23 kcal/mol), and only weakly exothermic for Pt ($\Delta H_{Pt} = -4$ kcal/mol).

From Table 2 it is evident that the highest activation energy associated with the progressive hydrogenation of carbon is that for the first step, $C_s + H_s \rightarrow CH_s$. The activation energies for subsequent steps decrease monotonically with the amount of hydrogen present in the CH_x group. This trend indicates that the most difficult step in the hydrogenation of surface carbon to methane is the formation of methyne groups, in agreement with recent experimental observations (*22–24*).

We should note, however, that there is a problem with the model since it projects (at least, for the zero-coverage limit) that the decomposition of methyne groups to carbon is an unactivated process. This pro-

jection seems to be inconsistent with the known formation of relatively stable CH species on a variety of metal surfaces (*25*). The result is particularly baffling because our calculated value of Q_{CH} = 90 kcal/mol for Ni(111) is indistinguishable from that obtained by the ab initio SCF-CI many-electron embedding theory (*26*). Of course, the lack of the barrier, $\Delta E^*_{CH} = 0$, should not be taken literally; there can be some barrier, say ΔE^*_{CH} = 5–10 kcal/mol (cf. the above discussion). At present, we have no clear means for explaining this problem.

The reaction pathway for forming CH_3OH is similar to pathway C in Figs. 1 and 2, with the exception that the CH_3O_s group undergoes hydrogenation rather than dissociation. As was noted earlier, for Pd the activation energy for CH_3O_s hydrogenation to CH_3OH is lower than the activation energy for CH_3O_s dissociation to $CH_{3,s}$ and O_s. This fact, together with the unfavorable energetics for C–O bond cleavage in earlier reaction steps, explains why CH_3OH can be synthesized over Pd. The formation of CH_3OH over Ni is far less favorable because the activation energy for CH_3O_s dissociation is lower than that for CH_3O_s hdyrogenation, and as a consequence the formation of CH_4 is preferred.

Our conclusion that the partial hydrogenation of CO can facilitate C–O bond dissociation is in agreement with experimental studies (*27–30*). Of particular interest here is the work of Mori *et al.* (*6, 28*) who studied the effects of metal composition on the H_2/D_2 isotope effect for hydrogenation of adsorbed CO to CH_4. They suggested the following mechanism of C–O bond dissociation,

$$(CO)_s \overset{H_s}{\rightleftarrows} (COH_n)_s \rightarrow (CH_x)_s + (OH)_s, \qquad x = n - 1.$$

Using transition-state theory they predicted that the magnitude of the isotope effect should increase with an increase in the number of hydrogen atoms (n) in $(COH_n)_s$. From a comparison of the predicted and observed magnitudes of the isotope effect they concluded that n is 1 for Fe, 2 for Ni, and 3 for Pd. Our results are consistent with those of Mori *et al.* (*6, 28*), indicating that hydrogen-assisted C–O bond cleavage will be more significant for Pd than for Ni.

Mechanistic studies of CO hydrogenation over Ni have shown that the specific reaction rates and the activation energies are practically the same for both Ni(111) and (100) single-crystal surfaces and for small supported Ni particles (*22–24*). The observation of a constant carbide coverage under reaction conditions over the temperature range 450–750 K suggests that the relevant specific rates of carbidic carbon formation and removal are very close and that the activation energy for carbide formation is nearly the same as that for carbide hydrogenation (*23b*). Our calculations support this conclusion. As may be seen from Table 2 and Figs. 1 and 2, the activation energies for CO_s dissociation and C_s hydrogenation are 67 and 63 kcal/mol, respectively. The calculations presented here indicate that both CH_4 and CH_3OH formation on Pd (and Pt) can proceed via the same elementary steps up to the formation of CH_3O_s, which may then undergo hydrogenation to form CH_3OH or decomposition to produce $CH_{3,s}$ and O_s, the activation energies for these processes being 18 and 23 kcal/mol, respectively. The similarity of the two activation energies is consistent with the fact that on Pd powder the selectivities to CH_4 and CH_3OH are approximately the same (~50% of each product (*31*)). For supported Pd catalysts the spread in CH_4 and CH_3OH selectivities is greater, reflecting the effects of Pd dispersion and support composition (*32–34*).

Finally, we comment on the decomposition of methanol CH_3OH_s on metal surfaces. From Table 3 (cf. also Figs. 1 and 2) it is evident that the formation of CH_3O_s and H_s is much more favorable than the formation of $CH_{3,s}$ and OH_s, in full agreement

with experiment (*35*). (By contrast, recent ab initio GVB calculations on Ni_{20} clusters, undertaken to simulate the chemisorption of CH_3OH on a Ni(100) surface, predict that the decomposition of CH_3OH to $CH_{3,s}$ and OH_s should be preferred (*36*). We also note that once formed, CH_3O_s should not decompose immediately to H_2CO, since there is an activation barrier for this process. Here, too, the predictions of our model are consistent with experimental observation (*17*).

CONCLUSIONS

A number of important insights into the mechanism of CO hydrogenation over Pt group metals can be obtained by using the bond-order-conservation method to calculate the total energies of adsorbed species and the activation barriers to their formation. Examination of the calculated energy profiles for CH_4 and CH_3OH synthesis over (111) surfaces of Ni, Pd, and Pt leads to the following conclusions. For Ni, cleavage of the C–O bond in chemisorbed CO occurs by direct dissociation ($S + CO_s \rightarrow C_s + O_s$). The subsequent reaction of C_s with H_s to form CH_4 ($C_s + 4H_s$) is an endothermic process. During the stepwise hydrogenation of C_s, the process with the highest activation energy is that leading to the formation of CH_s ($C_s + H_s \rightarrow CH_s$). The assistance of hydrogen in C–O bond cleavage appears to be critical for Pd and Pt. For these metals, the activation energy for direct CO dissociation is very high ($\geq$100 kcal/mol). BOC calculations suggest that the C–O bond is broken only after CO_s has been hydrogenated to CH_3O_s ($CH_3O_s \rightarrow CH_{3,s} + O_s$). Because the activation barriers for CH_3O_s dissociation to $CH_{3,s}$ and O_s and CH_3O_s hydrogenation to form CH_3OH are close, Pd and Pt are effective for both CH_4 and CH_3OH formation. Thus, the calculations based on the BOC approach explain the selectivities observed experimentally for CO hydrogenation over Ni, Pd, and Pt. These calculations also predict that CH_3OH decomposition on metal surfaces will take place via O–H bond cleavage (i.e., $CH_3OH \rightarrow CH_3O_s + H_s$) to produce CH_3O_s groups, in agreement with experimental observation.

APPENDIX

Partitioning of the total bond energy in a polyatomic molecule into two-center contributions has no physical significance and, therefore, makes sense only if it serves some practical purpose. One is therefore free to develop any working scheme to define the effective value of D_{AB} to best reproduce the experimental values of Q_{AB} and ΔE^*_{AB}, provided the *same* partitioning principle is used for all related polyatomic molecules. This principle involves averaging of chemical structures representing reasonable limits (upper and lower) of two-center bond energies. The scheme used in the present work is illustrated by the following two examples.

Let us consider the triatomic radical, HCO. In the gas phase, its total bond energy is $D_{HCO} = 274$ kcal/mol (see Table 1). We want to partition D_{HCO} into the sum of the C–H and C–O bond energies, namely

$$D_{HCO} = D_{HC} + D_{CO} = 274 \text{ kcal/mol}.$$

Taken separately, D_{CH} and D_{CO} are not observable and, therefore, cannot be uniquely defined. Intuitively, their meaningful values will be bound between two extremes corresponding to dissociations

$$HCO \rightarrow H + CO \quad \text{(A1)}$$

$$HCO \rightarrow HC + O \quad \text{(A2)}$$

For the gas-phase molecules CO and CH, the bond energies are $D_{CO} = 257$ kcal/mol and $D_{CH} = 81$ kcal/mol. Thus, the C–H and C–O bond energies in HCO may be assumed to be intermediate (III) between the two limiting structures (I and II), namely

$$\text{I}\quad H \overset{17}{—} C \overset{257}{—} O \leftrightarrow H \overset{81}{—} C \overset{193}{—} O \quad \text{II}$$

$$H \overset{D}{—} C \overset{274\text{-}D}{—} O \quad \text{III}$$

where the C–H bond energy $D_{CH} = D$ lies within the range $17 \leq D \leq 81$ kcal/mol.

In principle, D could be determined by using Eqs. (2)–(9) together with experimentally measured value of Q_{HCO}, $\Delta E^*_{H(CO)}$, or $\Delta E^*_{(HC)O}$. But, even if accurate values of Q and ΔE^* were available, this method of determining D would be inaccurate due to the approximate character of Eqs. (2)–(9) for polyatomic molecules. To avoid ad hoc fitting procedures, we have chosen to determine D by taking an arithmetic average of the values of D for structures I and II. Thus, $D = D_{CH} = \frac{1}{2}(17 + 81) = 49$ kcal/mol and $D_{CC} = \frac{1}{2}(257 + 193) = 225$ kcal/mol.

As the number of atoms in a polyatomic molecule increases, the choice of the limiting structures becomes an increasingly difficult task due to the larger number of conceivable reorganizations. For meaningful BOC calculations of the dissociation activation barriers, this chioce is critical because the limiting structures are averaged arithmetically. The approach we have used for polyatomic species can be illustrated for the case of CH_3O_s.

The gas-phase bond energy for CH_3O_s is $D_{H_3CO} = 383$ kcal/mol (see Table 1). We want to compare the dissociation routes

$$H_3CO \begin{cases} \longrightarrow H_3C + O & \text{(A3)} \\ \longrightarrow H_2CO + H & \text{(A4)} \end{cases}$$

and therefore, we should define the effective C–O and C–H bond energies in CH_3O. Since $D_{CH_3} = 293$ kcal/mol, the limiting structure for dissociation via reaction (A3) will be

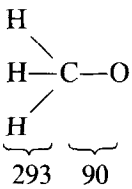

IV

and so $D_{CO} = 90$ kcal/mol. Another limiting value for D_{CO} can be taken from the bond energy portioning in CH_3OH. Since D_{CH_3OH}, D_{CH_3}, and D_{OH} are 487, 293, and 102 kcal/mol, respectively (see Table 1), we find $D_{CO} = 92$ kcal/mol, so the effective value of D_{CO} for reaction (A3) is $\frac{1}{2}(90 + 902) = 91$ kcal/mol.

Determination of the effective C–H bond energy is more complex. Since the total bond energy for formaldehyde is $D_{H_2CO} = 361$ kcal/mol, the limiting structure corresponding to dissociation via reaction (A4) will be

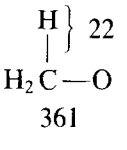

V

and hence $D_{CH} = 22$ kcal mol. On the other hand, the bond energy for CH in the gas phase is 81 kcal/mol. We can, therefore, envision a second limiting structure as

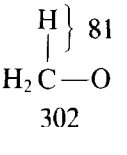

VI

By averaging, we obtain

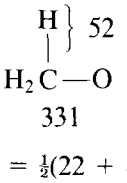

VII

Thus, $D_{CH} = \frac{1}{2}(22 + 81) = 52$ kcal/mol for dissociation via reaction (A4).

ACKNOWLEDGMENT

Alexis T. Bell acknowledges support of this work by the Division of Chemical Sciences, Office of Basic Energy Sciences, U.S. Department of Energy, under Contract DE-AC03-76SF00098.

REFERENCES

1. Ponec, V., *Catal. Rev.* **18,** 151 (1978).
2. Bell, A. T., *Catal. Rev.* **23,** 203 (1981).
3. Biloen, P., and Sachtler, W. M. W., "Advances in Catalysis" (D. D. Eley, P. W. Selwood, and P. B. Weisz, Eds.), Vol. 30, p. 165. Academic Press, San Diego, 1981.
4. Vannice, M. A., "Catalysis-Science and Technology," Vol. 3, Chap. 3. Springer-Verlag, West Berlin, 1982.
5. Anderson, R. B., "The Fischer–Tropsch Synthesis." Academic Press, San Diego, 1984.

6. Mori, T., Miyamoto, A., Niizuma, H., Takahashi, N., Hattori, T., and Murakami, Y., *J. Phys. Chem.* **90,** 109 (1986).
7. Takeuchi, A., and Katzer, J. R., *J. Phys. Chem.* **85,** 937 (1981).
8. Rabo, J. A., Risch, A. P., and Poutsma, M. L., *J. Catal.* **53,** 295 (1978).
9. (*a*) Shustorovich, E., *J. Amer. Chem. Soc.* **106,** 6479 (1984); (*b*) *Surf. Sci.* **150,** L115 (1985); (*c*) **163,** L645 (1985); (*d*) **163,** L730 (1985); (*e*) **175,** 561 (1986); (*f*) **176,** L863 (1986); (*g*) **181,** L205 (1987); (*h*) **187,** L627 (1987).
10. Shustorovich, E., *Surf. Sci. Rep.* **6,** 1 (1986).
11. Shustorovich, E., and Bell, A. T., *Surf. Sci.*, in press.
12. "CRC Handbook of Chemistry and Physics," 65th ed., pp. F171–190. CRC Press, Boca Raton, FL, 1984–85.
13. Frisch, M. J. personal communication to E. Shustorovich.
14. Brass, S. G., and Erlich, G., *Surf. Sci.* **187,** 21 (1987).
15. Fisher, G. B., and Gland, J. L., *Surf. Sci.* **94,** 446 (1980).
16. Madey, T. E., *in* "The Structure of Surfaces" (M. A. Van Hove and S. U. Tong, Eds.), pp. 264–268. Springer-Verlag, Berlin, 1985.
17. Hall, R. B., *J. Phys. Chem.* **91,** 1007 (1987).
18. Sexton, B. A., and Hughes, A. E., *Surf. Sci.* **140,** 227 (1984).
19. Anton, A. B., Parmenter, J. E., and Weinberg, W. H., *J. Amer. Chem. Soc.* **108,** 1823 (1986).
20. (*a*) Lee, M. B., Beckerle, J. D., Tang, S. L., and Ceyer, S. T., *J. Chem. Phys.* **87,** 723 (1987); (*b*) Ceyer, S. T., Beckerle, J. D., Lee, M. B., Tang, S. L., Yang, Q. Y., and Himes, M. A., *J. Vac. Sci. Technol. A* **5,** 501 (1987).
21. Goodman, D. W., Pebbles, D. E., and White, J. M., *Surf. Sci.* **140,** L239 (1984).
22. Goodman, D. W., *Acc. Chem. Res.* **17,** 194 (1984).
23. (*a*) Goodman, D. W., Kelley, R. D., Madey, T. E., and Yates, J. T., Jr., *J. Catal.* **63,** 226 (1980); (*b*) Goodman, D. W., Kelley, R. D., Madey, T. E. and White, J. M., *J. Catal.* **64,** 479 (1980); (*c*) Kelley, R. D., and Goodman, R. D., *Surf. Sci.* **123,** L743 (1982).
24. Yates, J. T., Jr., Gates, S. M., and Russel, J. N., Jr., *Surf. Sci.* **164,** L839 (1985).
25. See, for example, (*a*) Hills, M. M., Parmeter, J. E., Mulling, C. B., and Weinberg, W. H., *J. Amer. Chem. Soc.* **108,** 3554 (1986); (*b*) Seip, U., Tsai, M.-C., Kiippers, J., and Ertl, G., *Surf. Sci.* **147,** 65 (1984); (*c*) Stuve, E. M., and Madix, R. J., *J. Phys. Chem.* **89,** 105 (1985).
26. Whitten, J. L., private communication to E. Shustorovich. See also "Abstracts of Papers, 194th ACS Meeting, New Orleans, LA, Aug. 30–Sept. 4, 1987," Phys. 188.
27. Ho, S. V., and Harriott, P., *J. Catal.* **64,** 272 (1980).
28. (*a*) Mori, T., Masuda, H., Imai, H., and Murakami, Y., *Nippon Kagaku Kaishi,* 1449 (1979); (*b*) Mori, T., Masuda, H., Imai, H., Miyamoto, A., Baba, S., and Murakami, Y., *J. Phys. Chem.* **86,** 2753 (1982); (*c*) Mori, T., Masuda, H., Imai, H., Miyamoto, A., Hasabe, R., and Murakami, Y., *J. Phys. Chem.* **87,** 3648 (1983); (*d*) Miizuma, H., Hattori, T., Mori, T., Miyamoto, A., and Murakami, Y., *J. Phys. Chem.* **87,** 3652 (1983).
29. Wang, S.-Y., Moon, S. H., and Vannice, M. A., *J. Catal.* **71,** 167 (1981).
30. (*a*) Rieck, J. S., and Bell, A. T., *J. Catal.* **96,** 88 (1985); (*b*) **99,** 262 (1986).
31. Ryndin, Yu. A., Hicks, R. F., Bell, A. T., and Yermakov, Yu. I., *J. Catal.* **80,** 287 (1981).
32. Poutsma, M. E., Elek, L. F., Ibarbia, P. A., Risch, A. P., and Rabo, J. A., *J. Catal.* **52,** 168 (1978).
33. Fajula, F., Anthony, R. G., and Lunsford, J. H., *J. Catal.* **73,** 237 (1982).
34. Kikiuzono, Ya, Kagami, S., Naito, S., Onishi, T., and Tamura, K., *Discuss. Faraday Soc.* **72,** 135 (1981).
35. Canning, N. D. S., and Madix, R. J., *J. Phys. Chem.* **88,** 2437 (1984).
36. Upton, T. H., *J. Vac. Sci. Technol.* **20,** 527 (1982).